Moving Forward to Constrain the Shear Viscosity of QCD Matter

Gabriel Denicol,[1] Akihiko Monnai,[2] and Björn Schenke[1]
[1]Physics Department, Brookhaven National Laboratory, Upton, New York 11973, USA
[2]RIKEN BNL Research Center, Brookhaven National Laboratory, Upton, New York 11973, USA
(Received 15 December 2015; published 26 May 2016)

We demonstrate that measurements of rapidity differential anisotropic flow in heavy-ion collisions can constrain the temperature dependence of the shear viscosity to entropy density ratio η/s of QCD matter. Comparing results from hydrodynamic calculations with experimental data from the RHIC, we find evidence for a small $\eta/s \approx 0.04$ in the QCD crossover region and a strong temperature dependence in the hadronic phase. A temperature independent η/s is disfavored by the data. We further show that measurements of the event-by-event flow as a function of rapidity can be used to independently constrain the initial state fluctuations in three dimensions and the temperature dependent transport properties of QCD matter.

DOI: 10.1103/PhysRevLett.116.212301

Introduction.—The matter produced in ultrarelativistic heavy-ion collisions at the Relativistic Heavy Ion Collider (RHIC) and the Large Hadron Collider (LHC) has been shown to behave like an almost perfect fluid. It is well described by viscous relativistic hydrodynamics with one of the smallest shear viscosity to entropy density ratios, η/s, ever observed (see Refs. [1–3] for recent reviews). To date, most hydrodynamic simulations of heavy-ion collisions have assumed a temperature independent η/s which is then extracted from the measurements. However, it is well known that the η/s of quantum chromodynamic (QCD) matter cannot be constant [4,5]: it is expected to display a strong temperature dependence and have a minimum around the phase transition or crossover region —a behavior shared by many fluids in nature [6]. Understanding and quantifying this temperature dependence around the transition from hadronic matter to the quark-gluon plasma (QGP) is of fundamental importance, as it will reveal the true transport properties of QCD matter in the strong coupling regime.

Recent progress in the experimental precision and the study of new observables [7–9] has opened up the path towards a quantitative determination of the transport properties of fundamental QCD matter, particularly the extraction of the temperature dependence of the shear viscosity [9] and even the bulk viscosity [10,11]. At this point, most of the theoretical effort in this direction used simplified dynamical descriptions of the collision that simulate the evolution of the produced QCD matter only in the midrapidity region and neglect the dynamics and fluctuations in the longitudinal direction (along the beam line).

With the advent of $(3+1)$-dimensional event-by-event relativistic viscous fluid dynamic simulations [12–15], this limitation is removed and we have theoretical access to the entire spacetime evolution of the medium produced in heavy-ion collisions. This can be of particular importance to the extraction of transport coefficients since temperature (and baryon chemical potential) profiles of the medium vary in the longitudinal direction, such that particles produced with different momentum rapidities provide access to a range of varying medium properties, even at a fixed collision energy.

In this Letter we propose to make use of this fact to extract the temperature dependence of η/s from the rapidity dependence of experimental observables. We employ a hydrodynamic simulation with an initial state that describes fluctuations of both net-baryon and entropy density in all three spatial dimensions. We show that the rapidity dependence of the flow harmonic coefficients v_2 and v_3, which measure the azimuthal momentum anisotropy of the particles produced in the collision, is sensitive to the temperature dependence of η/s. We find that agreement with experimental data requires a strong temperature dependence of η/s at lower temperatures and a minimum value in the transition region that is considerably smaller than previous predictions made that assume a constant η/s. We also constrain the rate at which this transport coefficient can grow as the temperature becomes larger.

Previous calculations have generally not been able to describe the pseudorapidity dependence of v_2 [13,14,16,17]. The discrepancy was first attributed to deviations from equilibrium away from midrapidity in Refs. [16,18]. Indeed, our results indicate that the transport parameters and their temperature dependence are essential to achieving agreement with the data. We note, however, that the shape of the initial rapidity profile of the energy density, which is affected by longitudinal fluctuations [19–21], is also important. For example, while first results on the effect of temperature dependent transport parameters on the rapidity dependence of v_2 were presented in Ref. [14], both the lack of fluctuations and the choice of temperature dependent transport parameters likely contribute to the disagreement between calculations of the centrality and rapidity dependence of v_2 and the experimental data.

We further propose the measurement of the event-by-event distributions of the v_n as functions of rapidity to constrain the three-dimensional fluctuating initial state.

Initial state model and hydrodynamic evolution.—Initial state fluctuations in the transverse plane of the collision were discovered to be essential for the understanding of all observed multiparticle correlations [9,12,22–28]. In the fully three dimensional description of heavy-ion collisions, longitudinal fluctuations could have a similarly important effect [19–21]. Here, longitudinal fluctuations are introduced via a simple model that is a straightforward extension to the Monte Carlo Glauber model [29]. In this model, nucleons are sampled from Woods-Saxon distributions and constituent quarks from an exponential distribution [30] around the center of each nucleon. The quarks' longitudinal momentum fractions x are sampled from CT10 next-to-next-to-leading-order parton distribution functions [31] at $Q^2 = 1$ GeV^2 with EPS09 nuclear correction [32] using Les Houches Accord Parton Density Functions (LHAPDF6.1.4) [33]. Their initial rapidities are then given by $y_q = \pm y_{\mathrm{beam}} \mp \ln(1/x)$, where y_{beam} is the beam rapidity and the sign depends on whether the nucleus is right or left moving. According to a sampled impact parameter, two nuclei are then overlayed and wounded quarks determined using the quark-quark cross section σ_{qq}. We use Gaussian wounding [34,35] and $\sigma_{qq} =$ 9 mb for $\sqrt{s} = 200$ GeV collisions, which reproduces the nucleon-nucleon cross section of 42 mb.

The distribution of quarks in rapidity after the collision is determined using a Monte Carlo implementation of the Lexus model [36,37], where the probability of a quark with rapidity y_P obtaining rapidity y after collision with a quark of rapidity y_T (from the other nucleus) is

$$Q(y - y_T, y_P - y_T, y - y_P) = \lambda \frac{\cosh(y - y_T)}{\sinh(y_P - y_T)} + (1 - \lambda)\delta(y - y_P). \quad (1)$$

The parameter λ controls the degree of baryon stopping. In this Letter we use $\lambda = 0.22$, which reproduces the experimental net-baryon distribution in Au + Au collisions at $\sqrt{s} = 200$ GeV and lower collision energies. While each quark-quark collision changes both quarks' rapidity according to Eq. (1), an entropy density is deposited between the two quarks only for the last quark-quark collision. (Ordering of the collisions is done using the quarks' positions in the direction parallel to the beam line.) This method leads to number of quark participant scaling of the multiplicity. Entropy density is deposited in "tubes" around the center of mass of the two colliding quarks and is assumed to be constant in rapidity for each tube. The normalization of the entropy density for each tube is varied using negative binomial fluctuations, with the parameters adjusted to reproduce the measured multiplicity distribution. (This method is only approximate because the available experimental multiplicity distribution is uncorrected.) In the transverse plane, we smear the entropy density around the center of mass position of each pair by a Gaussian of width $\sigma_T = 0.2$ fm.

This model provides fluctuating entropy and baryon density profiles that are used as initial conditions for the hydrodynamic simulation MUSIC [12,28,38,39]. We use exactly the same setup as described in Ref. [37], except that we employ the relaxation time approximation to compute both bulk and shear nonequilibrium corrections to the particle distribution functions, leading to a linear dependence on the particle momentum [40].

The equation of state at finite baryon chemical potential is constructed by interpolating the pressures of hadronic resonance gas and lattice QCD [41,42] at the connecting temperature $T_c(\mu_B) = 0.166$ GeV $- 0.4(0.139$ GeV$^{-1}\mu_B^2 + 0.053$ GeV$^{-3}\mu_B^4)$. This ansatz is motivated by the chemical freeze-out curve determined in Ref. [43]. The temperature region below T_c can be interpreted as the hadronic phase, and the region above it as the QGP phase.

The initial time for the hydrodynamic evolution is $\tau_0 =$ 0.38 fm/c and kinetic freeze-out occurs at an energy density of 0.1 GeV/fm^3.

Temperature dependent transport parameters.—Similar to the investigations in Refs. [9,44,45], we employ a simple parametrization of the temperature dependent shear viscosity to entropy density ratio $(\eta/s)(T)$. Because we allow for finite baryon chemical potential μ_B, the more natural quantity to specify is $[\eta T/(\varepsilon + P)](T)$ [46]. At $\mu_B = 0$, this equals $(\eta/s)(T)$. For most rapidities in $\sqrt{s} = 200$ GeV collisions, μ_B is negligible, and we will use $\eta T/(\varepsilon + P)$ and η/s interchangeably in this Letter.

We assume a minimum at $T_c(\mu_B)$ and linear temperature dependencies above and below that minimum,

$$[\eta T/(\varepsilon + P)](T) = [\eta T/(\varepsilon + P)]_{\mathrm{min}} + a \times (T_c - T)\theta(T_c - T) + b \times (T - T_c)\theta(T - T_c), \quad (2)$$

where a and b are the slope parameters to be varied in the presented analysis.

We will study four scenarios. A constant transport parameter $\eta T/(\varepsilon+P)=0.12$; a large shear viscosity in the hadronic phase with $[\eta T/(\varepsilon+P)]_{\mathrm{min}}=0.04$, $a=10$, and $b=0$; a large viscosity in the QGP phase using $[\eta T/(\varepsilon+P)]_{\mathrm{min}}=0.04$, $a=0$, and $b=10$; and a large hadronic and moderate QGP viscosity using $[\eta T/(\varepsilon + P)]_{\mathrm{min}} =$ 0.04, $a = 10$, and $b = 2$. Figure 1 shows a comparison of $[\eta T/(\varepsilon + P)](T)$ in these four scenarios.

In all scenarios the shape of the bulk viscosity's temperature dependence is the same as employed in Ref. [11], where it is assumed to peak in the transition region. In this Letter the peak position is chosen to be at $T_c(\mu_B)$ and we replace the entropy density s by $(\varepsilon + P)/T$ to account for the finite baryon chemical potential. Note that the inclusion of bulk viscosity has been shown to be necessary to describe the mean transverse momentum of hadrons observed at the LHC for impact parameter dependent Glasma model (IP-Glasma) initial conditions [11]. We remark that the same conclusion holds for the initial state used in this Letter.

Rapidity spectra.—We present as a baseline the results for the pseudorapidity dependent particle spectra in comparison

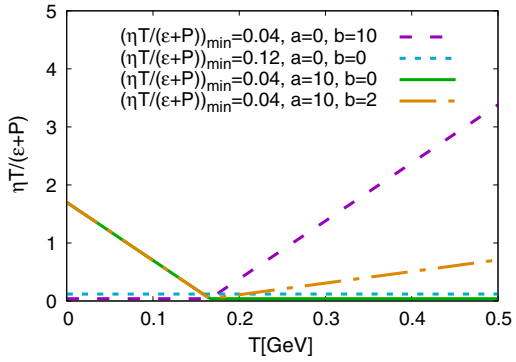

FIG. 1. The four scenarios of temperature dependent $\eta T/(\varepsilon + P)$ at $\mu_B = 0$.

to PHOBOS data [47] in Fig. 2. The normalization of the initial entropy density was adjusted in each scenario to fit the most central (0%–3% central) events. The dip around midrapidity is less pronounced than in models that use a flat rapidity plateau in the initial entropy density distribution [13]. A large viscosity at higher temperatures inhibits the longitudinal expansion most and leads to the best description of the spectra with the used initial state model. At $\eta_p = 4$, $dN/d\eta_p$ is overestimated by approximately 15% in the two scenarios with the smallest QGP viscosity.

Rapidity dependent anisotropic flow.—The flow harmonics v_n as functions of pseudorapidity are calculated using the event average,

$$v_n\{2\}(\eta_p) = \frac{\langle v_n v_n(\eta_p) \cos n[(\psi_n - \psi_n(\eta_p))]\rangle}{\sqrt{\langle v_n^2\rangle}}. \quad (3)$$

$\psi_n(\eta_p)$ is the event plane at pseudorapidity η_p, and v_n and ψ_n are the average values over the pseudorapidity range $|\eta_p| < 6$. We have verified that, in the simulation, the resulting $v_n\{2\}(\eta_p)$'s are very close to the root mean square values $\sqrt{\langle v_n^2(\eta_p)\rangle}$. For clarity of notation, in the following we will refer to $v_n\{2\}(\eta_p)$ from Eq. (3) as $v_n(\eta_p)$.

We show results for the charged hadron $v_2(\eta_p)$ for (top panel) 0%–40% and (bottom panel) 3%–15% and 15%–25% central $\sqrt{s} = 200$ GeV collisions and $p_T > 0.15$ GeV

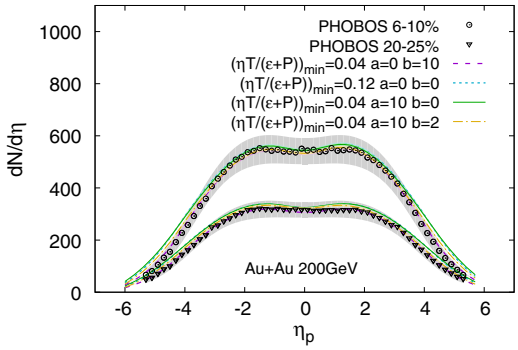

FIG. 2. $dN/d\eta_p$ of charged hadrons in two different centrality classes for the four scenarios compared to experimental data from the PHOBOS Collaboration [47].

in Fig. 3 for the four different scenarios discussed above. [All results for $v_n(\eta_p)$ were symmetrized around $\eta_p = 0$ to increase the statistics.] One can see that different temperature dependencies lead to variations in the η_p dependence. Because the average temperature decreases with increasing rapidity, a large hadronic shear viscosity causes $v_2(\eta_p)$ to drop more quickly with $|\eta_p|$, while a large QGP viscosity makes the distribution flatter in η_p. The constant $\eta T/(\varepsilon+P)$ case lies between the two cases. Previous calculations using UrQMD in the low temperature regime, which can be compared to the case of large hadronic viscosity, show a similar trend [17,20], although with a smaller effect.

The v_2 of charged hadrons as a function of pseudorapidity at the RHIC has been measured by the PHOBOS [48,49] and STAR [50] collaborations. As shown in Fig. 3, the existing data can already constrain the temperature dependence of $\eta T/(\varepsilon + P)$. Clearly, a large hadronic viscosity is favored by the PHOBOS data, while a constant value is hard to reconcile with the experimentally observed decrease of v_2 with pseudorapidity. Assuming that the initial state is not dramatically different from our model description, a QGP shear viscosity as large as the largest one used in this calculation can be excluded. We note that this scenario predicts a wrong centrality dependence of v_2 even at midrapidity. The scenario with large hadronic and moderate QGP shear viscosity is still compatible with most

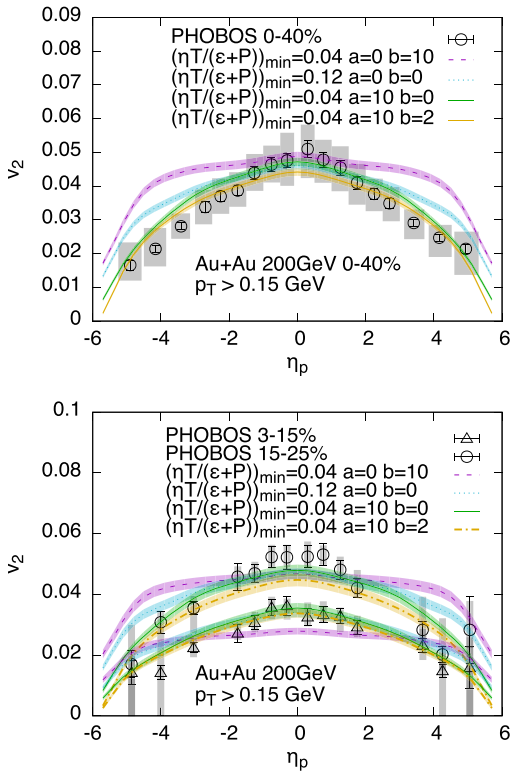

FIG. 3. v_2 of charged hadrons as a function of pseudorapidity for the four different shear viscosity scenarios compared to experimental data from the PHOBOS Collaboration [48,49]. (Top panel) 0%–40% centrality. (Bottom panel) 3%–15% and 15%–25% centralities.

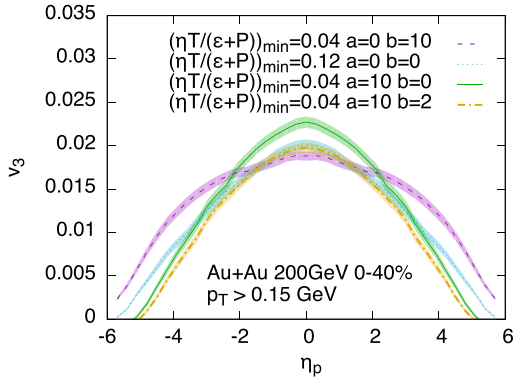

FIG. 4. Predictions for v_3 of charged hadrons as a function of pseudorapidity for the four scenarios.

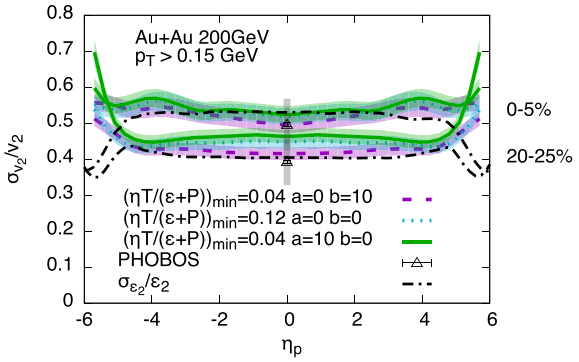

FIG. 5. Variance of the v_2 event-by-event distribution for different temperature dependent $\eta T/(\varepsilon + P)$'s. Dash-dotted lines are the scaled variances of the eccentricity distributions in the initial state. The data points represent PHOBOS data [55] for $N_{\text{part}} = 214$ (≈20%–25%) and 296 (≈0%–5%).

of the data, although slightly below around midrapidity in the 15%–25% central case.

We note that we find a larger effect of a large hadronic viscosity than in Ref. [13]. Possible reasons could be that (1) our shear viscosity is larger at low temperatures (75% larger at $T = 100$ MeV), and (2) the initial state employed here changes more quickly with rapidity compared to the constant rapidity plateau used in Ref. [13].

In Fig. 4 we show the prediction for the pseudorapidity differential triangular flow coefficient v_3. We see a faster drop than for v_2 with an increasing $|\eta_p|$. The measurement of this quantity can serve as a consistency check for the temperature dependence of η/s and can allow us to further constrain the three-dimensional fluctuating initial state.

As stated above, the experimentally observed shape of $v_2(\eta_p)$ demands a significant increase of $\eta T/(\varepsilon + P)$ with dropping temperature in the hadronic phase and, at the same time, only a mild increase—or none at all—with increasing temperature in the QGP phase. Note that increasing the hadronic viscosity will decrease the magnitude of the elliptic flow coefficient v_2 also at $\eta_p = 0$, a quantity that is already well described by theory. To compensate for this effect, the minimum value of η/s had to be reduced by a factor of 3 when compared to the case where an effective viscosity is used, i.e., $\eta/s = 0.12$. Hence, the true minimum of the QCD shear viscosity can be significantly smaller than what is predicted when extracting an effective temperature independent η/s. Within our framework, the largest value of the minimum consistent with the experimental data is $(\eta/s)_{\text{min}} \approx 0.04$ at zero baryon chemical potential, i.e., almost one half of the lower bound conjectured using the AdS/CFT duality [51,52].

Rapidity dependent v_n distributions.—At midrapidity, it was found that the v_n event-by-event distributions [53] are insensitive to the transport parameters of the medium (when scaled by the mean value) [54]. If this is also true at forward rapidities, the distributions could directly be used to constrain the initial state and its fluctuations in three dimensions. In Fig. 5 we show the (scaled) standard deviation of the v_2 distributions vs pseudorapidity $(\sigma_{v_2}/v_2)(\eta_p)$ in the first three scenarios for the shear viscosity temperature dependence. We also make a comparison to the scaled variances of the eccentricity distributions in the initial state. At the RHIC, this quantity has been measured at midrapidity by both PHOBOS [55] and STAR [56].

One can see that (1) at midrapidity the scaled variances are compatible with experimental data from PHOBOS [55], (2) there is almost no dependence on the pseudorapidity in any of the three cases, (3) final results are close to the initial state results over a wide range in rapidity, and (4) results are only weakly dependent on $\eta T/(\varepsilon + P)$. Thus, the measurement of cumulants of the v_n distributions (or the full distributions) as functions of rapidity will give important information about the 3D initial state and its fluctuations, largely independent of the transport parameters of the medium. It will be particularly interesting to compare predictions for such distributions from more sophisticated initial state models—such as the color glass condensate based IP-Glasma model [28,57,58] that is extended to three dimensions using Jalilian-Marian, Iancu, McLerran, Weigert, Leonidov, and Kovner evolution [59–63]—because they predict fluctuation scales that depend on rapidity [64,65].

Conclusions and outlook.—We have presented results from fully $(3 + 1)$-dimensional viscous relativistic hydrodynamic simulations including temperature dependent shear and bulk viscosities and using an initial state model that provides three-dimensional fluctuating baryon and entropy densities. We have shown that different scenarios for the temperature dependent $\eta T/(\varepsilon + P)$ can lead to significantly different results for the rapidity dependence of elliptic and triangular flow. A comparison with RHIC data has provided strong evidence that $\eta T/(\varepsilon + P)$ cannot be constant but must grow with decreasing temperature in the hadronic phase. The case of a strong increase of $\eta T/(\varepsilon+P)$ in the QGP phase $[\eta T/(\varepsilon + P)](400\ \text{MeV}) \approx 2.4$ is not compatible with the experimental data, while a moderate increase in the QGP $[\eta T/(\varepsilon + P)](400\ \text{MeV}) \approx 0.5$ cannot be excluded. Within our framework, we have determined

the minimum value to be $(\eta/s)_{\mathrm{min}} \approx 0.04$, almost one half of the lower bound conjectured using the AdS/CFT duality. We have shown that measurements of $v_3(\eta_p)$ can provide further constraints.

The event-by-event fluctuations of the flow harmonics are found to be almost insensitive to the transport parameters over a wide range of pseudorapidity and thus carry direct information on the fluctuating structure of the produced medium in all spatial dimensions. This calls for precise measurements of v_n and its fluctuations over wide ranges in rapidity and at different collision energies at the RHIC and the LHC. They have the potential to eliminate the large theoretical uncertainties in the longitudinal direction and to overconstrain the fluctuating initial state and the temperature dependent transport parameters of QCD matter.

A. M. is supported by the RIKEN Special Postdoctoral Researcher program. G. S. D. and B. P. S. are supported under U.S. DOE Contract No. DE-SC0012704. This research used resources of the National Energy Research Scientific Computing Center, which is supported by the Office of Science of the U.S. Department of Energy under Contract No. DE-AC02-05CH11231. B. P. S. acknowledges receipt of a DOE Office of Science Early Career grant.

[1] U. Heinz and R. Snellings, Annu. Rev. Nucl. Part. Sci. **63**, 123 (2013).
[2] C. Gale, S. Jeon, and B. Schenke, Int. J. Mod. Phys. A **28**, 1340011 (2013).
[3] R. D. de Souza, T. Koide, and T. Kodama, Prog. Part. Nucl. Phys. **86**, 35 (2016).
[4] M. Prakash, M. Prakash, R. Venugopalan, and G. Welke, Phys. Rep. **227**, 321 (1993).
[5] P. B. Arnold, G. D. Moore, and L. G. Yaffe, J. High Energy Phys. 05 (2003) 051.
[6] L. P. Csernai, J. I. Kapusta, and L. D. McLerran, Phys. Rev. Lett. **97**, 152303 (2006).
[7] A. Bilandzic, C. H. Christensen, K. Gulbrandsen, A. Hansen, and Y. Zhou, Phys. Rev. C **89**, 064904 (2014).
[8] G. Aad *et al.* (ATLAS Collaboration), Phys. Rev. C **90**, 024905 (2014).
[9] H. Niemi, K. J. Eskola, and R. Paatelainen, Phys. Rev. C **93**, 024907 (2016).
[10] J.-B. Rose, J.-F. Paquet, G. S. Denicol, M. Luzum, B. Schenke, S. Jeon, and C. Gale, Nucl. Phys. **A931**, 926 (2014).
[11] S. Ryu, J. F. Paquet, C. Shen, G. S. Denicol, B. Schenke, S. Jeon, and C. Gale, Phys. Rev. Lett. **115**, 132301 (2015).
[12] B. Schenke, S. Jeon, and C. Gale, Phys. Rev. Lett. **106**, 042301 (2011).
[13] P. Bozek, Phys. Rev. C **85**, 034901 (2012).
[14] E. Molnar, H. Holopainen, P. Huovinen, and H. Niemi, Phys. Rev. C **90**, 044904 (2014).
[15] I. A. Karpenko, P. Huovinen, H. Petersen, and M. Bleicher, Phys. Rev. C **91**, 064901 (2015).
[16] T. Hirano, Phys. Rev. C **65**, 011901 (2001).
[17] C. Nonaka and S. A. Bass, Phys. Rev. C **75**, 014902 (2007).
[18] T. Hirano, U. W. Heinz, D. Kharzeev, R. Lacey, and Y. Nara, Phys. Lett. B **636**, 299 (2006).
[19] R. P. G. Andrade, F. Grassi, Y. Hama, T. Kodama, and W. L. Qian, Phys. Rev. Lett. **101**, 112301 (2008).
[20] K. Werner, T. Hirano, I. Karpenko, T. Pierog, S. Porteboeuf, M. Bleicher, and S. Haussler, J. Phys. G **36**, 064030 (2009).
[21] L.-G. Pang, G.-Y. Qin, V. Roy, X.-N. Wang, and G.-L. Ma, Phys. Rev. C **91**, 044904 (2015).
[22] A. P. Mishra, R. K. Mohapatra, P. S. Saumia, and A. M. Srivastava, Phys. Rev. C **77**, 064902 (2008).
[23] J. Takahashi, B. M. Tavares, W. L. Qian, R. Andrade, F. Grassi, Y. Hama, T. Kodama, and N. Xu, Phys. Rev. Lett. **103**, 242301 (2009).
[24] B. Alver and G. Roland, Phys. Rev. C **81**, 054905 (2010).
[25] B. H. Alver, C. Gombeaud, M. Luzum, and J.-Y. Ollitrault, Phys. Rev. C **82**, 034913 (2010).
[26] H. Holopainen, H. Niemi, and K. J. Eskola, Phys. Rev. C **83**, 034901 (2011).
[27] Z. Qiu, C. Shen, and U. W. Heinz, Phys. Lett. B **707**, 151 (2012).
[28] C. Gale, S. Jeon, B. Schenke, P. Tribedy, and R. Venugopalan, Phys. Rev. Lett. **110**, 012302 (2013).
[29] M. L. Miller, K. Reygers, S. J. Sanders, and P. Steinberg, Annu. Rev. Nucl. Part. Sci. **57**, 205 (2007).
[30] R. Hofstadter, Rev. Mod. Phys. **28**, 214 (1956).
[31] J. Gao, M. Guzzi, J. Huston, H.-L. Lai, Z. Li, P. Nadolsky, J. Pumplin, D. Stump, and C. P. Yuan, Phys. Rev. D **89**, 033009 (2014).
[32] K. J. Eskola, H. Paukkunen, and C. A. Salgado, J. High Energy Phys. 04 (2009) 065.
[33] A. Buckley, J. Ferrando, S. Lloyd, K. Nordstrom, B. Page, M. Rufenacht, M. Schonherr, and G. Watt, Eur. Phys. J. C **75**, 132 (2015).
[34] A. Bialas and A. Bzdak, Acta Phys. Pol. B **38**, 159 (2007).
[35] W. Broniowski, M. Rybczynski, and P. Bozek, Comput. Phys. Commun. **180**, 69 (2009).
[36] S. Jeon and J. I. Kapusta, Phys. Rev. C **56**, 468 (1997).
[37] A. Monnai and B. Schenke, Phys. Lett. B **752**, 317 (2016).
[38] B. Schenke, S. Jeon, and C. Gale, Phys. Rev. C **82**, 014903 (2010).
[39] B. Schenke, S. Jeon, and C. Gale, Phys. Rev. C **85**, 024901 (2012).
[40] P. Bozek, Phys. Rev. C **81**, 034909 (2010).
[41] S. Borsanyi, Z. Fodor, C. Hoelbling, S. D. Katz, S. Krieg, and K. K. Szabo, Phys. Lett. B **730**, 99 (2014).
[42] S. Borsanyi, Z. Fodor, S. D. Katz, S. Krieg, C. Ratti, and K. Szabo, J. High Energy Phys. 01 (2012) 138.
[43] J. Cleymans, H. Oeschler, K. Redlich, and S. Wheaton, Phys. Rev. C **73**, 034905 (2006).
[44] H. Niemi, G. S. Denicol, P. Huovinen, E. Molnar, and D. H. Rischke, Phys. Rev. Lett. **106**, 212302 (2011).
[45] H. Niemi, G. S. Denicol, P. Huovinen, E. Molnar, and D. H. Rischke, Phys. Rev. C **86**, 014909 (2012).
[46] J. Liao and V. Koch, Phys. Rev. C **81**, 014902 (2010).
[47] B. Alver *et al.* (PHOBOS Collaboration), Phys. Rev. C **83**, 024913 (2011).

[48] B. B. Back *et al.* (PHOBOS Collaboration), Phys. Rev. Lett. **94**, 122303 (2005).
[49] B. B. Back *et al.* (PHOBOS Collaboration), Phys. Rev. C **72**, 051901 (2005).
[50] B. I. Abelev *et al.* (STAR Collaboration), Phys. Rev. C **77**, 054901 (2008).
[51] G. Policastro, D. T. Son, and A. O. Starinets, Phys. Rev. Lett. **87**, 081601 (2001).
[52] P. K. Kovtun, D. T. Son, and A. O. Starinets, Phys. Rev. Lett. **94**, 111601 (2005).
[53] G. Aad *et al.* (ATLAS Collaboration), J. High Energy Phys. 11 (2013) 183.
[54] H. Niemi, G. S. Denicol, H. Holopainen, and P. Huovinen, Phys. Rev. C **87**, 054901 (2013).
[55] B. Alver *et al.* (PHOBOS Collaboration), Phys. Rev. Lett. **104**, 142301 (2010).
[56] G. Agakishiev *et al.* (STAR Collaboration), Phys. Rev. C **86**, 014904 (2012).
[57] B. Schenke, P. Tribedy, and R. Venugopalan, Phys. Rev. Lett. **108**, 252301 (2012).
[58] B. Schenke, P. Tribedy, and R. Venugopalan, Phys. Rev. C **86**, 034908 (2012).
[59] J. Jalilian-Marian, A. Kovner, A. Leonidov, and H. Weigert, Nucl. Phys. **B504**, 415 (1997).
[60] J. Jalilian-Marian, A. Kovner, A. Leonidov, and H. Weigert, Phys. Rev. D **59**, 014014 (1998).
[61] E. Iancu, A. Leonidov, and L. D. McLerran, Nucl. Phys. **A692**, 583 (2001).
[62] E. Ferreiro, E. Iancu, A. Leonidov, and L. McLerran, Nucl. Phys. **A703**, 489 (2002).
[63] A. H. Mueller, Phys. Lett. B **523**, 243 (2001).
[64] A. Dumitru, J. Jalilian-Marian, T. Lappi, B. Schenke, and R. Venugopalan, Phys. Lett. B **706**, 219 (2011).
[65] S. Schlichting and B. Schenke, Phys. Lett. B **739**, 313 (2014).